scanning for motions up to 8mm (motion A), which can be further reduced to 2% if 10x rescanning is applied per field (see results of one example patient case in figure 1). For larger motions, given the same rescan#, volumetric re-scanning results in 5% better homogeneity than layered, but requires 6.5 times longer treatment time (for 700ms energy changes). Layered re-scanning can at best achieve homogeneity within about 10% of those of the static case, while volumetric rescanning gets to within 5%, but is extremely case and rescan# specific. By reducing the energy switching time, treatment times can decrease by 68% for volumetric re-scanning (100ms energy changes), but with no further improvements on D5-D95. Motion irregularity has pronounced influence only on the two large motions (B and C) but generally has more effect on volumetric re-scanning than layered re-scanning.
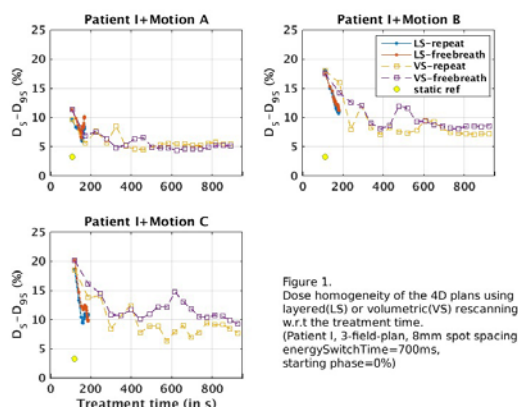

Figure 1.
Dose homogeneity of the 4D plans using layered(LS) or volumetric(VS) rescanning w.r.t the treatment time.
(Patient I, 3-field-plan, 8mm spot spacing energySwitchTime=700ms, starting phase=0%)

Conclusions: For larger motions, layered re-scanning has been shown to be the most time efficient, whereas volumetric rescanning is more effective for retrieving dose homogeneity. However, for motions below 8mm, both techniques are equally effective, particularly if multiple field plans are used. Taking into account realistic beam and scanning parameters for the Varian ProBeam system, and based on realistic and variable breathing patterns in different liver cases, our results indicate that re-scanning is a viable motion mitigation technique for this system, particularly if layered re-scanning is used.

OC-0549
Improving the clinical applicability of markerless lung tumour tracking with contrast-enhanced kV imaging
A. Fassi[1], D. Ciardo[2], M. Riboldi[1], D. Sarrut[3], G. Baroni[1]
[1]Politecnico di Milano, Dipartimento di Elettronica Informazione e Bioingegneria, Milano, Italy
[2]European Institute of Oncology, Department of Radiation Oncology, Milano, Italy
[3]CREATIS Centre Léon Bérard, Department of Radiotherapy, Lyon, France

Purpose/Objective: In-room kV imaging is widely applied for intrafraction motion compensation in image-guided radiation therapy (IGRT). The low contrast of lung tumours in kV images and the overlap of high-intensity surrounding structures, such as the mediastinum, may limit the applicability of IGRT techniques in lung cancer treatments. The aim of this study is to apply a CT-based contrast enhancement method to improve markerless lung tumour tracking in kV images, thus enhancing the potential of X-ray-based image guidance in lung cancer patients.
Materials and Methods: The contrast enhancement technique, previously proposed for cone-beam CT [1] and proton radiography [2], consists in subtracting to the original image a digital reconstructed radiograph (DRR) obtained by masking out the tumour from the planning CT volume. The target position is identified in the resulting contrast-enhanced (CE) image through template matching, by using as template the projection of the CT tumour volume. The application of the contrast enhancement technique to kV imaging was tested on a clinical dataset of lung cancer patients acquired with the CyberKnife Xsight Lung Tracking System (XLTS). The dataset include two patients (P1-P2) treated in three XLTS fractions and four patients (P3-P6) simulated with the XLTS but not treated, since the tumour was not visible in the stereoscopic kV images. A breath-hold CT scan was collected for each patient and five kV images per view were selected for each treatment fraction and simulation, considering for patients P1-P2 the images with the highest XLTS detection confidence.
Results: As shown in Figure 1, the contrast enhancement method allows tumour localization for all patients except P6, for whom the different diaphragm position in the breath-hold DRR and Live kV images hindered tumour visibility. The Michelson contrast [2] between the tumour and the surrounding structures was increased in the CE images by a factor of at least 2.2 compared to the Live images (Table 1). The median value of the ratio between the tumor contrast in CE images and in Live images was 4.9 and 8.6 for the lung and mediastinum background regions, respectively. For patients P1-P2, the absolute difference in the bidimensional tumour position identified with the XLTS and with the contrast enhancement technique ranged between 0.4 and 1.6 mm, with a median value of 1.2 and 1.0 mm for the horizontal and vertical image directions, respectively.
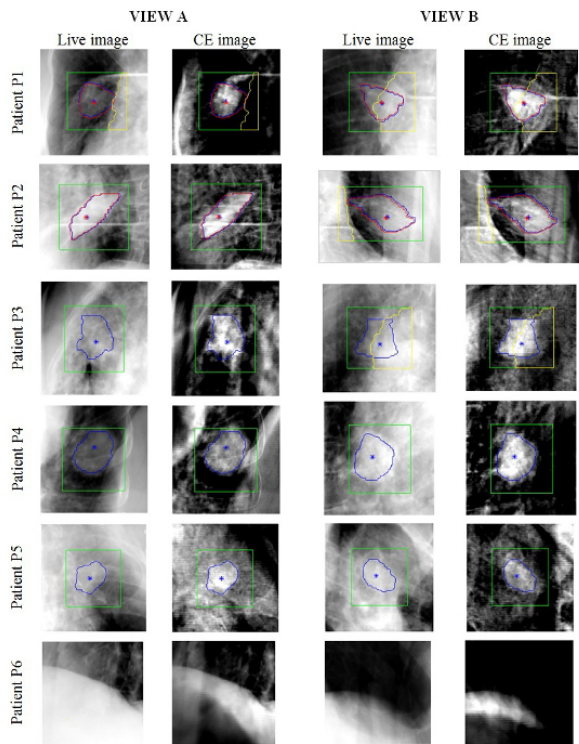
Figure 1. Examples of Live kV images acquired with the XLTS and corresponding CE images obtained for the two projection views of each patient. Tumour contours identified with the XLTS and with the contrast enhancement method are outlined in red and blue, respectively. Lung and mediastinum background regions used to compute the tumour contrast are depicted in green and yellow, respectively.

Table 1. Ratio between the Michelson contrast computed for the CE images and for the corresponding Live projections at different tumour-background interfaces. Results for each patient are expressed as median ± inter-quartile range of the contrast values obtained for all kV images selected in the simulation and treatment fractions.

Patient	$Contrast_{CE} / Contrast_{Live}$			
	VIEW A		**VIEW B**	
	Tumour-lung	Tumour-mediastinum	Tumour-lung	Tumour-mediastinum
P1	9.0 ± 11.1	7.6 ± 3.8	2.2 ± 0.3	8.6 ± 10.8
P2	2.2 ± 0.1	-	5.3 ± 0.6	-
P3	53.6 ± 262.7	-	2.9 ± 0.8	8.7 ± 4.0
P4	5.9 ± 0.5	-	9.8 ± 14.6	-
P5	6.3 ± 0.7	-	4.7 ± 0.4	-

Conclusions: The potential of the contrast enhancement method in increasing the applicability of markerless lung tumour tracking based on kV imaging was demonstrated on clinical data. A time-resolved (4D) CT scan can be used instead of the breath-hold CT scan available for this study in order to improve the robustness in the background subtraction operation, especially in case of lower lobe tumours for the compensation of diaphragm motion due to breathing.

[1] Yang Y *et al*, IJROBP 2012;82:e749-56.
[2] Spadea MF *et al*, IJROBP 2014;90:628-36.

OC-0550

Feasibility of markerless tumor tracking by sequential dual-energy fluoroscopy on a clinical tumor tracking system

J. Dhont[1], K. Poels[1], D. Verellen[1], K. Tournel[1], M. Boussaer[1], C. Collen[1], B. Engels[1], T. Gevaert[1], F. Steenbeke[1], M. De Ridder[1]

[1]Universitair Ziekenhuis Brussel, Radiotherapy, Brussels, Belgium

Purpose/Objective: The purpose of this study is to evaluate the feasibility of markerless tumor detection using sequential dual-energy fluoroscopy sequences. As fast-switching kilovolt (kV) generators are not readily available, motion artifacts due to a time lapse between high and low energy images are often a cause for concern. For those kV generators without rapid switching, an alternative approach is proposed consisting of using sequential (high and low kV) high frame rate fluoroscopy sequences, already available in the clinical dynamic tracking (DT) workflow of the Vero SBRT system to build the hybrid correlation model.

Materials and Methods: Two sequential 20s (11 Hz) fluoroscopy sequences were acquired at the start of one fraction for 4 patients treated for primary NSCLC with DT on the Vero SBRT system. Two sequences were acquired, using 2 on-board kV imaging systems located at ± 45° from the MV beam axis, at respectively 60 kV (3.2 mAs) and 120 kV (2.0 mAs). Table 1 shows the kV imager positions, which were selected based on marker visibility. Offline, a normalized cross-correlation algorithm was applied to anatomically match the high (HE) and low energy (LE) images. Per breathing phase (inhale, exhale, maximum inhale and maximum exhale), the five best matching HE and LE couples were extracted for dual energy subtraction. A validation on an anthropomorphic phantom with an imposed artificial tumor volume was conducted to validate the dual-energy approach. A contrast analysis according to gross tumor volume (GTV) was conducted between the DE and HE images based on contrast to noise ratio. Improved tumor visibility was quantified in function of 4 breathing phases using an improvement ratio ($IR = CNR_{DE} / CNR_{HE}$).

Results: The additional acquisition of a 60 kV fluoroscopy sequence enabled an unambiguous approach to dual-energy imaging into the clinical workflow. Normalized cross correlation for HE-LE fluoroscopy sequence matching resulted in a mean correlation coefficient of 0.92 ± 0.18 based on the 5 best anatomical HE-LE matches per breathing phase. Contrast to noise ratio's (CNR) per patient can be found in Table 1. Bone suppression by DE subtraction imaging was successful. An example is shown in Figure 1. Based on the CNR, with the exception of one imaging angle the DE images showed no significantly improved tumor visibility compared to the HE images, with an improvement ratio averaged over all patients of 1.00 ± 0.50.
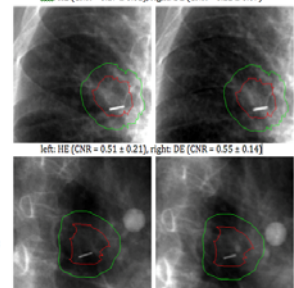
Conclusions: Dual-energy subtraction imaging by sequential orthogonal fluoroscopy was shown feasible by implementing an additional LE fluoroscopy sequence into the DT workflow. However, for most imaging angles, dual-energy images showed no significantly improved tumor visibility over HE imaging.

Table 1 Contrast to noise ratio and improvement ratio according to gross tumor volume (GTV) between the dual and high-energy images per patient.

	CNR SD		Improvement ratio
	HE	DE	
patient 1 Im. 1 - 35°	0.53 ± 0.15	0.21 ± 0.08	0.41 ± 0.10 p = 0.057
patient 1 Im. 2 - 125°	0.23 ± 0.08	0.40 ± 0.11	1.87 ± 0.63 p = 0.323
patient 2 Im. 1 - 225°	0.17 ± 0.02	0.12 ± 0.07	0.68 ± 0.42 p = 0.090
patient 2 Im. 2 - 315°	0.51 ± 0.21	0.55 ± 0.14	1.14 ± 0.28 p = 0.833
patient 3 Im. 1 - 315°	0.49 ± 0.14	0.63 ± 0.11	**1.42 ± 0.56** **p < 0.005**
patient 3 Im. 2 - 45°	1.07 ± 0.28	0.66 ± 0.05	0.65 ± 0.19 p = 0.005
patient 4 Im. 1 - 78°	0.22 ± 0.08	0.11 ± 0.09	0.57 ± 0.64 p = 0.009
patient 4 Im. 2 - 348°	0.85 ± 0.24	0.99 ± 0.11	1.24 ± 0.26 p = 0.021

Abbreviations: CNR = contrast to noise ratio; SD = standard deviation; HE = high energy; DE = dual energy

Figure 1 Dual energy subtraction images from patient 2, imager 1 (above) and imager 2 (below) (GTV = red contour). left: HE (CNR = 0.17 ± 0.02), right: DE (CNR = 0.12 ± 0.07)

left: HE (CNR = 0.51 ± 0.21), right: DE (CNR = 0.55 ± 0.14)

OC-0551

High spatial and timing resolution silicon based dosimeter for quality assurance of real time adaptive radiotherapy

M.K. Newall[1], M. Petasecca[1], M. Duncan[1], A.H. Aldosari[1], K. Al shukaili[1], C.S. Porumb[1], I. Fuduli[1], J.T. Booth[2], E. Colvill[2], P. Keall[3], M.L.F. Lerch[1], V. Perevertaylo[4], A.B. Rosenfeld[1]